

Automated numerical characterization of dilute semiconductors per comparison with luminescence

YANG, X., ORIAKU, C.I., ZUBELLI, J.P. and PEREIRA, Mauro
<<http://orcid.org/0000-0002-2276-2095>>

Available from Sheffield Hallam University Research Archive (SHURA) at:

<https://shura.shu.ac.uk/14809/>

This document is the Published Version [VoR]

Citation:

YANG, X., ORIAKU, C.I., ZUBELLI, J.P. and PEREIRA, Mauro (2017). Automated numerical characterization of dilute semiconductors per comparison with luminescence. *Optical and Quantum Electronics*, 49 (3). [Article]

Copyright and re-use policy

See <http://shura.shu.ac.uk/information.html>

Automated Numerical Characterization of Dilute Semiconductors per Comparison with Luminescence

X. YANG¹, C.I. ORIAKU², J.P. ZUBELLI¹ AND M.F. PEREIRA^{3,*}

¹*Instituto de Matematica Pura e Aplicada, Rio de Janeiro, 22460-320, Brazil*

²*Department of Physics Michael Okpara University of Agriculture, P.M.B. 7267, Nigeria*

³*Materials and Engineering Research Institute, Sheffield Hallam University, Sheffield, S1 1WB, UK*

**email: m.pereira@shu.ac.uk*

Abstract - This paper combines analytical approximations for the optical absorption and luminescence of semiconductors with Trust Region-Reflective (TRR) methods methods, delivering a robust numerical characterization method to be used in the study of new bulk semiconductors per direct comparison with experimental spectra. It further extends recent applications of the theory to the case of dilute nitride semiconductors and confirms results for the s-shape of the luminescence peak as a function of temperature.

Keywords: semiconductors; dilute nitrides; luminescence; mid infrared; many body effects

1 Introduction

The study of new semiconductor materials is important from a fundamental science point of view and for the ever increasing number of applications in optoelectronics. Concrete progress requires accurate and simple modelling that can predict optical properties and become a tool for numerical characterization and device design from the ultra-violet to the THz range and Mid Infrared Ranges [1-5]. Furthermore, understanding the properties of new bulk semiconductors has attracted renewed interest in the solar cell material arena to avoid environmentally unfriendly materials such as Cd [6].

The importance of the Coulomb interaction leading to many body and correlation effects is now a well-established fact from bulk to quantum dots and the associated nonlinear effects become significantly pronounced when a semiconductor is highly excited with light fields or electrically injected carriers [7]. Strong light fields create electron-hole pairs, which in turn constitute quantum mechanical many body systems interacting in various ways, e.g. band gap renormalization, band filling and Coulomb enhancement, screening and dephasing arising from the attractive and repulsive scattering processes from electrons, holes, phonons and impurity defects. At low temperatures and small carrier densities, excitonic effects dominate the optical absorption of bulk semiconductors and the excitons are bleached as the temperature and excitation densities increase due to a combination of screening, band filling and dephasing effects. But even at higher temperatures and densities, the Coulomb interaction is important [7] and plasma theories have delivered excellent approximations for the absorption and gain in this case and have been successfully applied to different isotropic bulk materials [8] and superlattices treated as effective anisotropic media [9,10]. Photoluminescence is crucial to characterise new materials and devices under development and this paper combines analytical approximations for the optical absorption and luminescence of semiconductors with Trust Region-Reflective (TRR) methods methods, delivering a robust numerical characterization method to be used in the characterisation of new bulk semiconductors per

direct comparison with experimental spectra. It further extends recent applications of the theory [11] to the case of dilute nitride semiconductors and confirms results for the s-shape of the luminescence peak as a function of temperature.

2 Mathematical Formalism

An interesting feature of dilute semiconductor material is the anomalous energy emission peaks at low temperatures, following an unusual s-shape behaviour that is associated with disorder and localization effects, which have been seen in both dilute bismides [12] and nitrides [3]. A simple and efficient method to describe this and other light emission effects in those materials is used here [11], based on analytical solutions for the Photon Green's functions approach [13,14,15], delivering a microscopic, fully quantum mechanical solution. Note that, in spite of its success to accurately explain experiments such as both single beam and nonlinear pump-probe photoluminescence [15], as well as being a powerful tool to design optical devices and solar cells [16]. The general

Nonequilibrium Green's Functions (NEGF) techniques that include Photon Green's functions mentioned above and semiconductor Bloch equations, can be applied to both intersubband [17-19] and interband transitions [20-21], but usually requires intensive numerical methods. Therefore, in this project, we did not fully calculate the dephasing attributed to electron-phonon, electron-impurity and electron-alloy disorder scattering and that leads to measured s-shape-like features in dilute semiconductor samples [22-23]. The scattering processes cited above can all be described by selfenergies [24,25,9]. Instead, we used Trust Region-Reflective (TRR) methods [26] to obtain the values of carrier density, homogeneous and inhomogeneous broadening that best characterize experimental results and as a future step, we shall

use these numbers to compare and contrast with Nonequilibrium Green's Functions (NEGF) calculations to help determine the relative influence of each scattering/dephasing mechanisms.

The quantum mechanical Poynting vector describing light emission can be expressed in terms of the Photon Green's Function, leading to the optical power density spectrum, which can be directly compared with photoluminescence experiments [11].

$$I(\omega) = \frac{I_0}{1+\exp(\beta(\hbar\omega-\mu))} \left\{ \sum_{n=1}^{\sqrt{g}} \frac{4\pi}{n} \left(\frac{1}{n^2} - \frac{n^2}{g^2} \right) \delta_{\Gamma}(\xi - e_n) + 2\pi \int_0^{\infty} \frac{\sinh(\pi g \sqrt{x})}{\cosh(\pi g \sqrt{x}) - \cos(\sqrt{4g-g^2}x)} \delta_{\Gamma}(\xi - x) dx \right\}, \quad (1)$$

where $I_0 = \frac{\hbar\omega^2 e^2 |\Pi|^2}{\pi e_0 c^3 a_0^3}$, $e_{n=-(n^{-1}-ng^{-1})^2}$, $\xi = (\hbar\omega - E_g)/e_0$, $g = (\kappa a_0)^{-1}$ and a_0, e_0 denote, respectively the exciton Bohr radius and binding energy.

Fluctuations in the alloy composition are described here by a Gaussian distribution in the dilute Bi mole fraction x . If x_0 is the nominal Bi mole fraction, and $I(x, \omega)$ is the expression in Eq. 8, the inhomogeneously broadened spectrum reads

$$I_{inh}(\omega) = \frac{1}{\sqrt{2\pi}\sigma} \int_{x_0-3\sigma}^{x_0+3\sigma} I(x, \omega) e^{-\left(\frac{x-x_0}{\sigma}\right)^2} dx \quad (2)$$

Thus, in order to compare our calculations with experimental data, we need three main parameters: the carrier density, the inhomogeneous broadening parameter and the homogeneous dephasing: (ρ, σ, Γ) .

2 Numerical Method and Results

In our model, $u_T(\rho, \sigma, \Gamma)$ is the luminescence peak energy function at temperature T . In the cases that we have investigated, the carrier density, inhomogeneous and homogeneous broadening are restricted to the following intervals (normalized units are used here) $\rho \in [1.5 \times 10^{14}, 10^{17}]$, $\sigma \in [10^{-3}, 2.5 \times 10^{-3}]$ and $\Gamma \in [1, 2]$.

Experimental data such as in Refs. [3,12] provides the luminescence peak energy at different temperatures for InAsN. Thus, by applying the least squares method, we can estimate the parameters (ρ, σ, Γ) so that the residual between the theoretical function and the experimental data is minimized. Since the scales of the parameters are different by several orders of magnitude, we introduce auxiliary variables, $\hat{\rho} = \log(\rho)$, $\hat{\sigma} = 10^4 \sigma$, $\hat{\Gamma} = 10\Gamma$. That leads to a trasformed function, $u_T(\rho, \sigma, \Gamma) = \hat{u}_T(\hat{\rho}, \hat{\sigma}, \hat{\Gamma})$. Ref. [3] provides a series of data points $d = (d_1, d_2, \dots, d_N)$ measured at $T = (T_1, \dots, T_N)$. Therefore, the problem becomes:

$$\min_{x=(\rho, \sigma, \Gamma)} \sum_{i=1}^N (\hat{u}_{t_i} - d_i)^2. \quad (3)$$

In order to address this problem, we selected the function `lsqnonlin` in Matlab, which applies Trust Rion-Reflective (TRR) methods. Compared with other techniques, such as line-searching methods, TRR delivers more accurate and less time costly results. In a nutshell, the reasoning underlying the TRR approach is as follows: Suppose we wish to minimize $F(x)$. In order to find a point x_{i+1} with a smaller function value, we proceed by minimizing the following quadratic model:

$$\min_{s \in N} m(s) = g^T s + \frac{1}{2} s^T H s, \quad (4)$$

where N is a neighbourhood of x_i and is called the trust region. g and H are the gradient and Hessian of F .

particular, $s \in N$ is equivalent to $\|D_i s\| < \Delta_i$, where D_i is a diagonal scaling matrix and Δ_i is a positive scalar. Then the current point is updated to $x_i + s$ if $F(x_i + s) < F(x_i)$; otherwise, the current point remains unchanged, ($x_{i+1} = x_i$), the region of trust is shrunk and the trial step computation is repeated. In other words, we set the new step size $\Delta_{i+1} \in (0, \tau \Delta_i]$, given a scaling factor $0 < \tau < 1$.

In order to solve for s in Eq. (4), there are several good algorithms. However, they require time proportional to several factorisations of H . Therefore, for trust-region problems, a more efficient approach is needed. The approximation approach followed in Optimization Toolbox solvers is to restrict the trust-region subproblem to a two-dimensional subspace S [27, 28]. Once the subspace S has been computed, the work to solve Eq. (4) is trivial even if full eigenvalue/eigenvector information is needed, since in the subspace, the problem is only two-dimensional. The dominant work has now been shifted to the determination of the subspace.

The two-dimensional subspace S is determined with the aid of a pre-condition conjugate gradient described below. The solver defines S as the linear space spanned by s_1 and s_2 , where s_1 is the direction of the gradient g and s_2 is either an approximate Newton direction, i.e., a solution to

$$H \cdot s_2 = -g, \quad (5)$$

or a direction of negative curvature,

$$s_2^T \cdot H \cdot s_2 < 0. \quad (6)$$

The philosophy behind this choice of S is to force global convergence (via the steepest descent directive or negative curvature direction) and achieve fast local convergence (via the Newton step, when it exists).

In our Numerical Experiments for Ref. [12], confirming the results found in Ref [11], the initial values for (ρ, σ, Γ) were $[1E15, 2E-3, 1]$. After 9 iterations, the

trust region shrank and the optimal values remained the same with the initial. These initial values were obtained by try and error during several runs. Therefore, we conclude that the local minimum for the function is found.

Figures 1 and 2 show results of the comparison between theory and experiments in Ref. [3], extending the findings of Ref. [11] for the InAsN case.

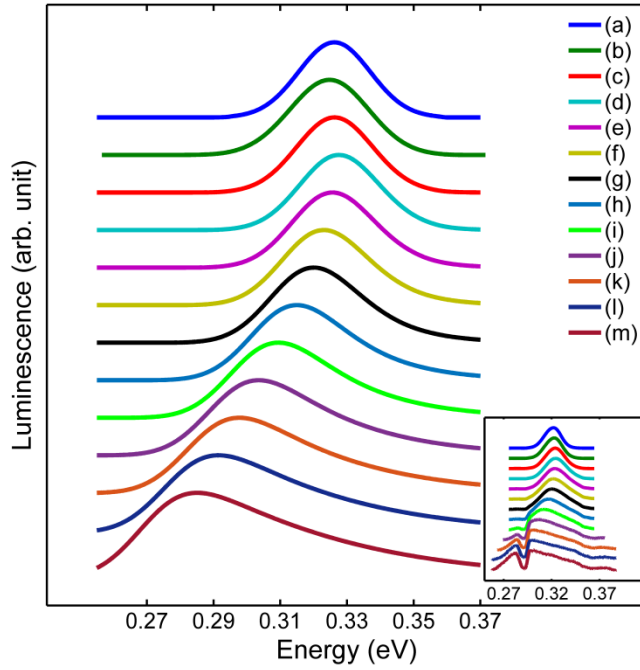


Fig.1 Theoretical vs Experimental (inset) luminescence for a InAsN sample at various temperatures. From (a) to (m) the temperatures are: 4, 20, 40, 60, 80, 100, 120, 150, 180, 210, 240, 270 and 300K . The low energy feature (around 0.28 meV) at high temperatures is due to the presence of CO2 in the optical path of the measurements. The experimental data for comparison has been extracted from [3] Krier et al. The density used in the calculations is $N=10^{14}$ carriers/cm³.

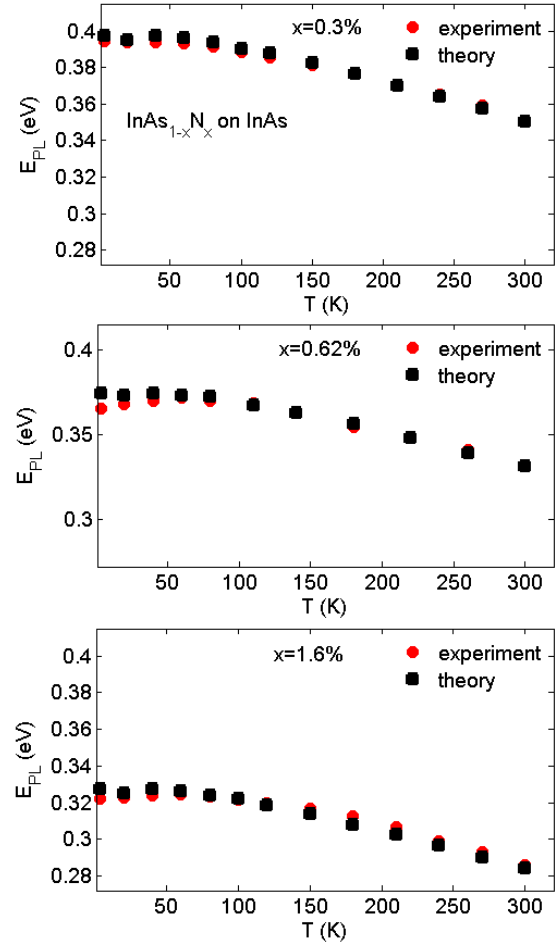


Fig.2 Plot of peak PL energy E_{PL} (eV) vs T (K) for the mole fractions (a) $x=0.3\%$ (b) $x=0.62\%$ (c) $x=1.6\%$ of $\text{InAs}_{1-x}\text{N}_x$ on InAs, Good agreement can be observed between the theory (black) and experiments from [3] A Krier, et al. The carrier density used is $n=10^{15}$ cm⁻³.

It is interesting to see that lower quality interfaces lead to more scattering and thus to a more pronounced s-shape as shown in Fig.3 where InAsN is grown on GaAs.

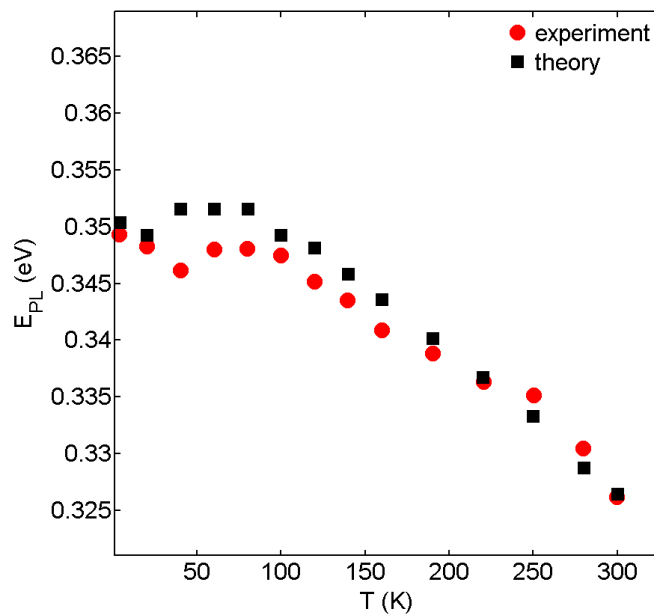


Fig.3 Plot of peak PL energy E_{PL} (eV) vs T (K) for $\text{InAs}_{1-x}\text{N}_x$ on GaAs. The experimental data has been extracted from Ref. [3]. Good agreement can be observed between the theory (black) and experiments from [3] A Krier, et al. The carrier density used is $n=10^{15}\text{cm}^{-3}$.

References

1. Jepsen P.U., Cooke D.G., Siegel P.H.: Introduction to the special issue on terahertz spectroscopy, IEEE Transactions On Terahertz Science And Technology **3**(3), 237-238 (2013).
2. Gu Y., Wang K., Zhou H., Li Y., Cao C., Zhang L., Zhang Y., Gong Q., Wang S.: Structural and optical characterizations of InPBi thin films grown by molecular beam epitaxy. Nanoscale Research Letters **9**(1), 24-24 (2014)
3. Krier A., De la Mare M., Carrington P.J., Thompson M., Zhuang Q., Patané A., Kudrawiec R.: Development of dilute nitride materials for mid-infrared diode lasers. Semicond. Sci. Technol. **27**, 4009-4009 (2012)

In summary, the automated numerical method developed validated our previous work that took days of trial and error attempt for a single data set. It can now be applied to a number of new materials, serve as guideline to interpret experimental data and to guide the choice of microscopic models that better deliver agreement with experiments. The comparison with experiments for the InAsN nitride case further validates our method as a powerful tool to support the characterization and development of new materials and devices.

Acknowledgements: The authors acknowledge support from COST ACTION MP1204, TERA-MIR Radiation: Materials, Generation, Detection and Applications.

4. De la Mare M., Zhuang Q., Krier A., Patané A., Dhar S.: Growth and characterization of InAsN/GaAs dilute nitride semiconductor alloys for the midinfrared spectral range. Applied Physics Letters **93**(3), 031110 (2009)
5. Zhuang Q., Godenir Q., Krier A., Tsai G., Lin H.H.: Molecular beam epitaxial growth of InAsN:Sb for midinfrared Optoelectronics. Applied Physics Letters **93**(12), 121903 (2008)
6. Vidal J., Botti S., Olsson P., Guillemoles J.F., Reining L.: Strong interplay between structure and electronic properties in $\text{CuIn}(\text{S}, \text{Se})_2$: a first-principles study. Phys. Rev. Lett. **104**(5), 056401 (2010)
7. Chemla D.S., Shah J.: Many-body and correlation effects in semiconductors. Nature **411**(6837), 549-557 (2001)

8. Banyai L, Koch S.W.: A simple theory for the effects of plasma screening on the optical-spectra of highly excited semiconductors. *Z. Phys. B* **63**(3), 283-291 (1986)
9. Pereira M.F.: Analytical solutions for the optical absorption of semiconductor superlattices. *Physical Review B* **52**(3), 1978-1983 (1995)
10. Pereira M.F.: Anisotropy and nonlinearity in superlattices. *Optical and Quantum Electronics* **48** (6), 1-7 (2016a)
11. Oriaku C.I., Pereira M.F.: Analytical solutions for semiconductor luminescence including Coulomb correlations with applications to dilute bismides, *J. Opt. Soc. Am. B* **34**, 321-328 (2017).
12. Mazzucato, S., Lehec, H., Carrère, H., Makhloufi, H., Arnoult, A., Fontaine, C., Amand, T., Marie, X.: Low-temperature photoluminescence study of exciton recombination in bulk GaAsBi. *Nanoscale Research Letters*, **9**(1), 1-5 (2014)
13. Pereira M.F., Henneberger K.: Green's functions theory for semiconductor-quantum-well laser spectra. *Phys. Rev. B* **53**(24), 16485-16496 (1996)
14. Pereira M.F., Henneberger K.: Microscopic theory for the influence of Coulomb correlations in the light-emission properties of semiconductor quantum wells. *Phys. Rev. B* **58**(4), 2064-2076 (1998)
15. Michler P., Vehse M., Gutowski J., Behringer M., Hommel D., Pereira M.F., Henneberger K.: Influence of Coulomb correlations on gain and stimulated emission in (Zn,Cd)Se/Zn(S,Se)/(Zn,Mg)(S,Se) quantum-well lasers, *Phys. Rev. B* **58** (4), 2055-2063 (1998)
16. Aeberhard U.: Theory and simulation of quantum photovoltaic devices based on the non-equilibrium Green's function formalism. *J. Comput. Electron.* **10**(4), 394-413 (2011)
17. Pereira Jr, M.F.: Microscopic approach for intersubband-based thermophotovoltaic structures in the terahertz and mid-infrared. *JOSA B* **28**(8), 2014-2017 (2011)
18. Pereira M.F., Faragai I.A.: Coupling of THz radiation with intervalence band transitions in microcavities. *Optics Express* **22**(3), 3439-3446 (2014)
19. Pereira, M. F.: The linewidth enhancement factor of intersubband lasers: from a two-level limit to gain without inversion conditions. *Applied Physics Letters* **109** (22), 222102-1 - 222102-4 (2016)
20. Pereira M. F., Binder R., Koch S.W.: Theory of nonlinear optical absorption in coupled-band quantum wells with many-body effects. *Applied physics letters* **64**(3), 279-281 (1994)
21. Grepel, H., Diessel A., Ebeling W., Gutowski J., Schüll K., Jobst B., Hommel D., Pereira M.F., Henneberger K.: High-density effects, stimulated emission, and electrooptical properties of ZnCdSe/ZnSe single quantum wells and laser diodes. *physica status solidi (b)* **194**(1), 199-217 (1996)
22. Imhof, S., Thränhardt, A., Chernikov, A., Koch, M., Köster, N.S., Kolata, K., Chatterjee, S., Koch, S.W., Lu, X., Johnson, S.R., Beaton, D.A.: Clustering effects in Ga (AsBi). *Applied Physics Letters*, **96**(13), 131115 (2010)
23. Kesaria, M., Birindelli, S., Velichko, A.V., Zhuang, Q.D., Patanè, A., Capizzi, M., Krier, A.: In (AsN) mid-infrared emission enhanced by rapid thermal annealing. *Infrared Physics & Technology*, **68**, 138-142 (2015)

24. Wacker A., Semiconductor superlattices: a model system for nonlinear transport. *Physics Reports* **357**(1), 1-111 (2002)
25. Schmielau, T., Pereira Jr. M.F.: Nonequilibrium many body theory for quantum transport in terahertz quantum cascade lasers., *Applied Physics Letters* **95**(23), 231111-1 - 231111-14 (2009)
26. Hung J., Energy Optimization of a Diatomic System. (2012).
27. Branch, M.A., Coleman T.F., Li Y.: A sub-space, interior, and conjugate gradient method for large-scale bound- constrained minimization problems. *SIAM Journal on Scientific Computing*, **21**(1), 1-23 (1999)
28. Byrd R.H., Schnabel R.B., Shultz G.A.: Approximate solution of the trust region problem by minimization over two-dimensional subspaces. *Mathematical Programming* **40**(1-3), 247-263 (1988)